Current trends and future directions in turbulent thermal convection

Ke-Qing Xia[a)]
Department of Physics, The Chinese University of Hong Kong, Shatin, Hong Kong, China

(Received 15 August 2013; accepted 2 September 2013; published online 10 September 2013)

Abstract The system of turbulent thermal convection is introduced. Progresses in recent decades in the four major areas of research in turbulent convection are briefly reviewed. Some of the recent trends of the field are then discussed, which also serve to point out that the future directions in this important field of fluid mechanics lie in the extension to the non-standard or non-classical Rayleigh–Bénard configuration. © *2013 The Chinese Society of Theoretical and Applied Mechanics.* [doi:10.1063/2.1305201]

Keywords turbulence, thermal convection, turbulent heat transport, thermal plumes, large-scale flow, small-scale turbulence

I. INTRODUCTION

Thermally-driven convective turbulent flows, or turbulent thermal convections is the most common type of turbulent flows occurring in nature. Examples include those in the stars, in the atmosphere and the liquid core of planets. Turbulent thermal convection is also important in many engineering applications in which heat transfers are involved. For this reason, turbulent convection has attracted the attention from researchers in a diverse array of fields, ranging from astrophysics and geophysics to mechanical engineering. Because the temperature and velocity fields are dynamically coupled to each other, i.e., thermal and mechanical energies are converted to each other over a wide range of length and time scales, the temperature field becomes an active scalar. This coupling makes convective turbulence a much richer and also much more complicated phenomenon than Navier–Stokes turbulence. A paradigm for turbulent convection is the classical Rayleigh–Bénard (RB) system, a fluid layer heated from below and cooled from the top. As a closed system with well-defined boundary conditions and precisely-tunable parameters, it is an idealized model to study turbulent flows involving heat transport and has attracted much attention during the past few decades.[1–6] As a system with many flow states ranging from simple oscillatory motion, transition to chaos, chaotic motion, soft and hard turbulence, it is also the most-studied model in nonlinear dynamics. The system is characterized by two control parameters: the Rayleigh number Ra and Prandtl number Pr, which are defined as

$$Ra = \frac{\alpha g \Delta T H^3}{\nu \kappa}, \tag{1}$$

and

$$Pr = \frac{\nu}{\kappa}, \tag{2}$$

respectively. Here α is the thermal expansion coefficient, ν the kinematic viscosity, and κ the thermal diffusivity of the convecting fluid, g is the gravitational acceleration, ΔT is the temperature difference between the bottom and the top plates, and H is the height of the fluid layer between the plates. In addition, the aspect ratio $\Gamma = D/H$ (D is the lateral dimension of the system) also plays an important role in the structures and dynamics of the flow. The state of motion in a thermally driven convecting fluid is governed by the Boussinesq equations, plus the incompressibility condition

$$\frac{\partial \boldsymbol{v}}{\partial t} + \boldsymbol{v} \cdot \nabla \boldsymbol{v} = -\frac{1}{\rho}\nabla p + \nu \nabla^2 \boldsymbol{v} + g\alpha\delta T \hat{\boldsymbol{z}}, \tag{3}$$

$$\frac{\partial T}{\partial t} + \boldsymbol{v} \cdot \nabla T = \kappa \nabla^2 T, \tag{4}$$

$$\nabla \cdot \boldsymbol{v} = 0. \tag{5}$$

In the above the first equation is essentially the Navier–Stokes equation with a buoyancy term. It is obtained under the so-called Oberbeck–Boussinesq approximation, which assumes that all material parameters of the fluid are independent of temperature and pressure. Only when considering the buoyancy term, is the temperature dependence of the density ρ taken into account in a linear approximation, i.e., $\rho = \rho_0(1-\alpha\delta T)$, where $\rho_0 = \rho(T_0)$ and $\delta T = T - T_0$ with T_0 being a reference temperature, which is usually taken as the mean temperature of the bulk fluid. When these equations are written in non-dimensional form, only the two control parameters Ra and Pr will be present in the equations of motion for the temperature and velocity fields. A measure of the heat transfer efficiency by convective flow is the Nusselt number $Nu = J/(\chi\Delta T/H)$, which is the ratio between the actual convective heat transfer (the flux J) and the heat that would be transferred if there exists only conduction, here χ is the thermal conductivity of the working fluid in quiescent state. The second response parameter is the well-known Reynolds number Re. Therefore, the system has three control parameters (Ra, Pr, and Γ) and two response parameters (Nu and Re). Figure 1 shows a cartoon of turbulent thermal convection with the main coherent structures

a)Corresponding author. Email: kxia@phy.cuhk.edu.hk.

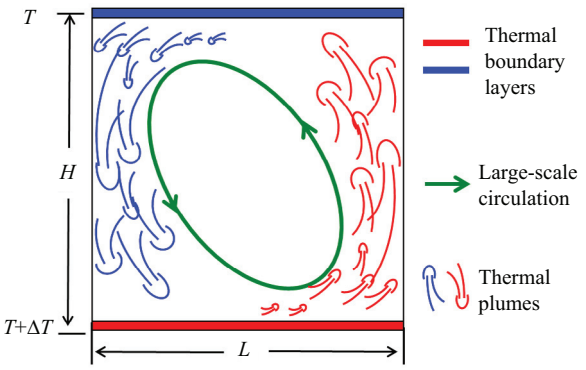

Fig. 1. A schematic drawing of turbulent RB convection that shows the major coherent structures in the system: thermal plumes and the large-scale circulation (LSC), as well as the boundary layers at the top and bottom plates. The drawing shows a two-dimensional system of aspect ratio one, but could also represent a vertical cross-section of a three-dimensional system in either cylindrical or rectangular geometries.

of the system: thermal plumes, the large-scale circulation (LSC), and the thermal boundary layers.

There are four major directions in the studies of convective thermal turbulence: turbulent heat transfer, boundary layer dynamics, coherent structures and flow dynamics, and small-scale turbulence. The progresses made in the past decade in the first three areas, i.e., heat transfer, boundary layers, and flow dynamics have been reviewed in detail in the recent article by Ahlers et al.[3] The progresses and current status on the small-scale properties of the velocity and temperature fields have been reviewed by Lohse and Xia.[4] In this article, I will give only a brief introduction and summary on the status of the major issues. Because of the space limit, my focus will be mainly on experimental studies. I will then present and discuss some of the progresses made since these reviews and focus on several future trends in this field.

II. TURBULENT HEAT TRANSFER

One of the most important issues in the study of turbulent thermal convection is to determine how heat is transported by highly turbulent flows and to understand why it is so. Here, one asks how the Nusselt number Nu depends on the three control parameters of the system at very high levels of turbulence, i.e., what is the functional form of $Nu(Ra, Pr, \Gamma)$? A number of theoretical models have been proposed over the years. The one proposed by Grossmann and Lohse (GL)[7–10] is arguably the most successful one. The key ingredient of this model is the decomposition of the kinetic energy and thermal dissipation rates into boundary layer (BL) and bulk contributions. It can adequately describe the behavior of Nu over a wide range of Ra and Pr. For very large Ra and small to moderate Pr, an earlier model proposed by Kraichnan[11] predicts that turbulent flow will enter an asymptotic state in which the boundary layers will become turbulent so that heat will be transported "ballistically" by turbulent flows. This implies that heat transfer will no longer be limited by molecular diffusivities, i.e., J will be independent of ν and κ. From dimensional analysis, one can immediately obtain that Nu should have an Ra-scaling with an exponent of $1/2$ (apart from a logarithmic correction). This asymptotic state later became known as the ultimate state of turbulent thermal convection. In the GL model this ultimate regime is also predicted as one of several states, depending on the parameter range of Ra and Pr. To either prove or disprove the existence of this ultimate regime is important because if it exists we can then, presumably, extrapolate results from laboratory experiment to convection phenomena occurring in astrophysical objects. Convections in astrophysical, and also in geophysical systems, typically have Ra larger than 10^{20}, a value that is beyond the reach of any laboratory experiment in the foreseeable future. In addition, new physics may be expected in this ultimate regime. There is no exact value for the onset Ra for this regime and it depends on the Prantal number. For $Pr \sim 1$ (the value for most gaseous fluids), estimates put this value at around 10^{13}–10^{14}. So far most of the very high Ra experiments are those made with low temperature helium gas because of its extremely low viscosity in low temperature.[12–14] However, several experiments made under nominally similar conditions appear to give contradictory results. As the helium gas is operated not far from its critical point, it is often not possible to maintain constant Pr while changing the Rayleigh number. So many of the low temperature helium experiments were not conducted under constant Pr which makes it difficult to disentangle the effects of Ra and Pr in the measured Nu.

Recently, He et al.[15] have reported observing the transition to this ultimate regime of thermal convection in an experiment over the Rayleigh number range $10^{12} \leqslant Ra \leqslant 10^{15}$ and at nearly constant Pr. They achieved this by using pressurized gas in the Gottingen high-pressure convection facility. For $Ra \leqslant 10^{13}$, these authors' measurements gave a relation $Nu \sim Ra^{\gamma_{\rm eff}}$ with $\gamma_{\rm eff} \approx 0.31$, which is consistent with the so-called classical RB convection. In an intermediate transition region ($10^{13} \leqslant Ra \leqslant 5\times10^{14}$), $\gamma_{\rm eff}$ experiences a gradual increase and within which multiple-stable states were also observed. When Ra is further increased beyond 5×10^{14} and up to $Ra = 10^{15}$ (the highest Ra reached in their experiment), these authors found that $\gamma_{\rm eff} = 0.38$. This is apparently consistent with the ultimate state with turbulent boundary layers predicted by Kraichnan. The value of $\gamma_{\rm eff} = 0.38$, rather than 0.50, is a result of the logarithmic correction. In the original Kraichnan model this logarithmic correction is also present in the Reynolds number (Re) dependence of Ra, but is absent in the more recent model for turbulent thermal convection by Grossmann and Lohse. In the same

experiment, He et al. indeed found $Re \sim Ra^{0.5}$ for $Ra > 5 \times 10^{14}$. (This was achieved with the help of the elliptic model,[16–19] as Taylor's frozen flow hypothesis does not apply in this case.) Therefore, their claim of observing a transition to the ultimate regime is further supported by the Reynolds number scaling. Furthermore, their results could differentiate the two models and appear to support the modified ultimate state predicted by the Grossmann and Lohse model. On the other hand, the experimental data of He et al. in this new regime only span about half decade of Ra, which makes their results less conclusive. As the transition to the ultimate state is essentially a transition of the boundary layers from being laminar to being turbulent, by directly looking for transitions in the boundary layers in future studies will provide more insight into this regime. Turbulent convection in the absence of BLs is known as homogeneous RB convection. In a numerical study Lohse and Toschi[20] have shown that in this case Nu indeed has a scaling $Ra^{0.5}$ as in the ultimate regime.

The Nusselt number dependence on the Prandtl number, the other control parameter of the system, is very important for model differentiations because different models have rather different predictions for the relation $Nu \sim Pr^{\alpha}$. For example, Kraichnan[11] has predicted that $\alpha = 0$ for $Pr > 0.1$; Shraiman and Sigga[21] predicted $\alpha = 0$; Grossmann and Lohse[7,8] on the other hand predicted that different regions in the Ra–Pr phase diagram have different values of α. In addition, the large Pr behavior of Nu may be relevant to problems like mantle convection. As the Prandtl number is determined by the fluid properties, it can only be varied over a very narrow range once a fluid is chosen. On the other hand, as can be seen from above, although different models predict different $Nu \sim Pr$ relations, the dependence on Pr is not strong, which means that in order to distinguish the different predictions one needs to vary Pr over a wide range. This may be illustrated by the experiment of Ahlers and Xu,[22] who found that Nu is decreased by about 2%–3% when Pr is increased from 4 to 34 (shown in Fig. 2). But the authors also pointed out that systematic errors could not be ruled out for the small drop which makes their results inconclusive. Therefore, only over a wide range of Pr can a relationship between Nu and Pr be established with certainty. This usually led to the comparison between data obtained from different experiments conducted with different convection cells (sometimes of different geometries). But this procedure inevitably introduces uncertainties to the interpretation of the data, since different experiments may be subjected to different systematic errors. By using a combination of several fluids, Xia et al.[23] measured Nu over two decades of Pr. As shown in Fig. 2, the trend that Nu decreases with increasing Pr is established unambiguously only over an extended range of Pr. Since Nu in Fig. 2 decayed about 20% over the varying range of Pr of the experiment, it can be concluded that Nu does decrease with increasing Pr for the parameter range of the experiment. This

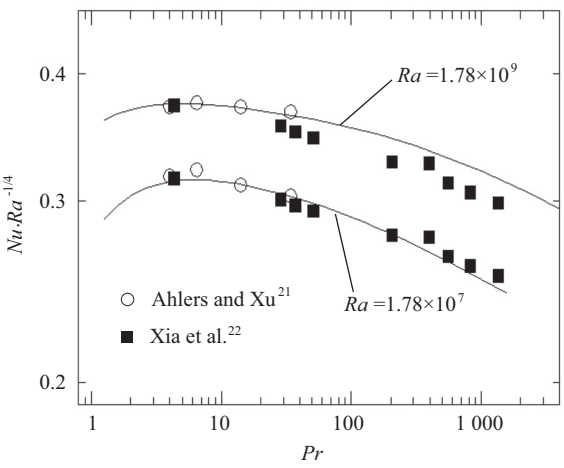

Fig. 2. Comparison between experimental data and the theoretical prediction of Grossmann and Lohse.[8] (Figure taken from Ref. 8)

conclusion is incompatible with the long standing prediction made by Kraichnan[11] that Nu is independent of Pr in the high Pr (> 0.1) and moderate Ra regime. It is also clear that both the experimental data of Xia et al.[23] and those of Ahlers and Xu[22] have excellent agreement with the prediction of the GL model. This agreement is now widely considered as a great success of the GL model.

All laboratory experiments are confined. Therefore the aspect ratio of system comes into play. By studying the aspect ratio dependence of the various flow properties, one hopes to gain an understanding on how confinement influences the turbulent flow, which may help one to extrapolate the knowledge gained in the confined case to the large aspect-ratio or un-confined situations such as those occurring in nature. A dominant flow structure in RB convection is the so-called large-scale circulation. While different flow structures are indeed observed in convection cells of different Γ,[24,25] high-precision Nu measurements have shown that it has a weak and in general non-systematic dependence on Γ in both cylindrical and rectangular cells.[26–30] As Γ has a strong influence on the flow structures, this also suggests an insensitivity of heat transport to the LSC.[3] Regarding the large Γ limit, in an experimental study of turbulent convection in a one-meter diameter convection cell over widely varying aspect ratios, Sun et al.[28] found that when $\Gamma > 10$, the asymptotic regime of lager Γ may have been reached. On the other hand, in the small Γ limit, i.e., increasing the effect of confinement, Huang et al.[31] recently found, unexpectedly, an increase of Nu. In Sect. VI (D), we will explain how this can happen.

III. BOUNDARY LAYER DYNAMICS

Boundary layers have long been recognized as playing a vital role in fluid mechanics systems. An obvious difference between convective thermal turbulence and other types of turbulence, such as turbulent shear flows, is that it has two types of boundary layers: the thermal boundary layer and the viscous boundary layer, and the two are dynamically coupled to each other. Measurement of the viscous boundary layer is very important for understanding the mechanism of turbulent flows in the system, since different models all have similar predictions for the scaling behavior between Nu and Ra, but have very different assumptions for the boundary layer. Because of the existence of strong temperature fluctuations, the measurement of viscous boundary layer in thermal turbulence has long been a challenge. Using a novel light scattering technique,[32] Xin et al.[33] made a direct measurement of the viscous boundary layer at the bottom plate in a cylindrical convection cell and found that the BL thickness $\delta_u \sim Ra^{-0.16}$. This result does not support the assumption of a classical turbulent boundary made by Shraiman and Siggia[21] in their model of thermal convection. At the sidewall of a cubic cell, however, Qiu and Xia[34] found that the viscous BL thickness follows the classical Prandtl–Blasius (PB) scaling. In a later study using particle image velocimetry (PIV), Sun et al.[25] measured the viscous BL at the bottom plate in a rectangular cell and found that δ_u also follows the classical PB scaling. This confirms the assumption of a PB boundary layer made in the GL model. Recently, Wei and Xia[35] made a PIV measurement of the viscous BL in a cylindrical cell and found that the difference between the results from Xin et al.[33] and Sun et al.[25] may be explained by the presence of the azimuthal motion of the LSC in the cylindrical cell and that when this azimuthal motion is suppressed the BL scaling in the cylindrical cell approaches that of the classical PB type.

While the Blasius-type laminar boundary condition is indeed a good approximation, in time-averaged sense, both in terms of its scaling and its various dynamical properties,[25] the shape of the velocity profile in turbulent convection is found to deviate[25,36] from that predicted by the PB boundary layer theory. Recently, Zhou and Xia[37] discovered that the intermittent ejection of thermal plumes leads to the fluctuations of the BL thickness and that the statistical properties of the BL fluctuations inside and outside the BL are different. As a result, a measurement position in the laboratory frame will be sometimes inside and sometimes outside the BL, which results in a mixed statistics in the measured time-averaged quantities. By introducing a dynamic scaling method that expresses the measured boundary layer quantities in a time-dependent frame that co-moves with the fluctuating boundary layer thickness itself, a clean separation between the two types of statistics is achieved and the measured velocity profile, when sampled in the time-dependent frame, is brought into perfect collapse with the theoretical PB profile. In a later study Zhou et al.[38] further showed that this dynamical method works not only for viscous BL but also for thermal BL, as well as for different Prandtl numbers. An example is shown in Fig. 3. This discovery prompted a number of subsequent studies on the boundary layer structures in turbulent convection. These studies show that, to varying degrees, the dynamical scaling method works in cells of different geometries and at different positions along the horizontal plates. But in general, the dynamically sampled profiles have better agreement with PB profile in 2D and quasi-2D cells than in 3D cases.[39–43] This is partly because the PB boundary layer theory is essentially a 2D model and partly because of the azimuthal motion of the LSC in the 3D case.[35]

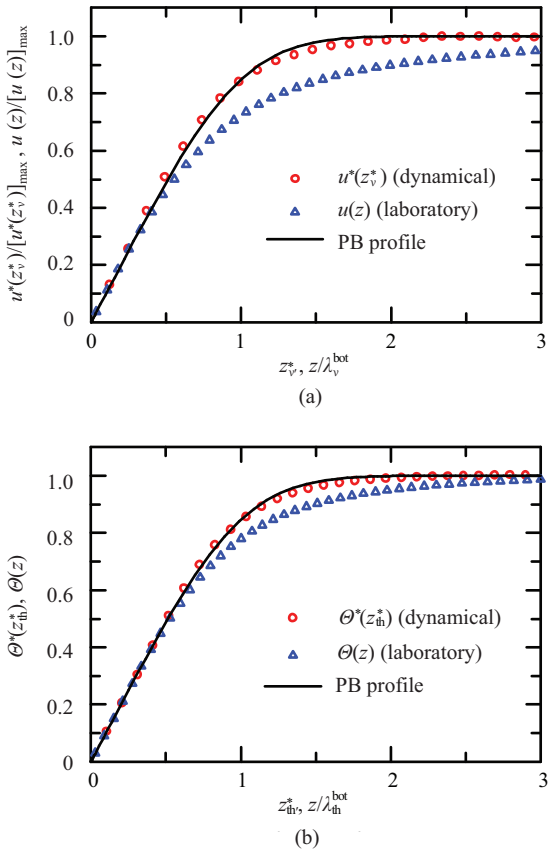

Fig. 3. Comparison between (a) velocity profiles and (b) temperature profiles near the bottom plate ($Ra = 10^9$ and $Pr = 0.7$).[38] (Figure taken from Ref. 38)

IV. COHERENT STRUCTURES

A. Large-scale flow dynamics

A fascinating feature of turbulent RB convection is the emergence of a well-defined and nearly coherent circulating roll spanning the height of the convection cell (for $\Gamma \simeq 1$), in defiant of the turbulent background. This LSC is also known as the wind of turbulent convection. An important question concerns the origin of

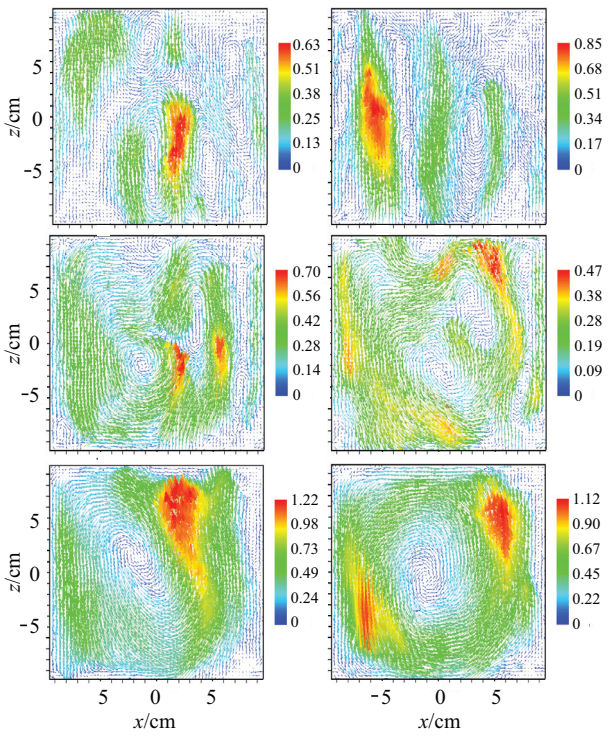

Fig. 4. PIV-measured velocity fields showing the formation of the LSC as a result of plume clustrering and organization.[44] (Figure taken from Ref. 44)

the LSC and its sustentation. To answer these questions, Xi et al.[44] studied the transient behaviour of the large-scale mean flow through both shadowgraph visualization of the thermal plumes and PIV measurements of the velocity field. Their experiment revealed that the fluid entrainment caused by the plume's vertical motion generates vortices surrounding the plume itself. These vortices in turn generate the initial horizontal motion of the flow field. It demonstrates clearly that it is the thermal plumes that initiate and sustain the horizontal large-scale flow. The velocity fields acquired by the particle image velocimetry shown in Fig. 4 illustrate various stages of the transient process of LSC formation, from straight-going starting plumes to plumes in a circulatory motion.

An important issue in the study of flow dynamics is the scaling of the Reynolds number Re with Ra, i.e., $Re \sim Ra^{\gamma}$. A riddle exists concerning the scaling exponent γ, a large number of experiments have produced a range of its value from 0.42 to 0.5. The difference is large enough that it can not be explained by experimental uncertainties and differences in the techniques used.[45] Because the properties of Re reflect the underlying driving mechanism and energy budget, this discrepancy is naturally a cause of concern.[9] Sun and Xia[46] analyzed results from various studies and found that the measured Re can be divided into two groups: one based on the circulation frequency of the mean wind and the other based on a directly measured velocity. For the first type of measurements, $Re_{\rm f} = u_{\rm LSC}H/\nu = 4H^2 f_{\rm C}/\nu$. A key step in Sun and Xia's work is the recognition that in the above formula the LSC has been implicitly assumed to have a constant circulation pathlength $\ell_{\rm LSC} = 4H$, whereas, as pointed out by Niemela and Sreenivasan,[47] $\ell_{\rm LSC}$ is not a constant but evolves with Ra. Sun and Xia[46] further measured the evolution of $\ell_{\rm LSC}$ with Ra and found that $\ell_{\rm LSC} = 4H$ only for sufficiently large Ra. This implies that the measured Re-scaling exponent is an effective exponent, i.e., $Re_{\rm f} = Ra^{\gamma_{\rm eff}}$. For the second type of measurements, Sun and Xia found that the inclusion of counterflows reduces the average velocity and changes the characteristic magnitude of the circulation speed of the wind. In fact, when flows in both directions become equally probable, the mean velocity will be close to zero. This means that a properly chosen wind velocity used to define a characteristic Reynolds number should not include the counterflow. When these factors are properly accounted for, both groups give $\gamma = 0.5$, which implies that a single mechanism is driving the flow for both low and high values of Ra.

As a coherent large-scale structure, the LSC has many intriguing dynamic features, such as azimuthal rotations and occasional cessations (momentary vanishing of its circulation speed) and reversals (of its circulation directions). Perhaps most striking among these is the coherent three-dimensional bulk oscillation, which has been observed in both the temperature and velocity measurements,[12,48,49] and in convection systems with different fluids[12,50,51] and different geometries.[24,52,53] In addition to the apparent oscillations observed for temperature and velocity in the vertical circulation plane of the LSC, horizontal oscillations of the velocity field have also been observed.[54–56] Villermaux[57] has suggested that this oscillation is a result of the periodic emission of thermal plumes from the boundary layers that are coupled by the LSC. His model assumes that plume emission from one plate is triggered by the arrival of thermal plumes from the other one, so that plumes are emitted not only periodically but also alternately between the top and bottom plates. Although some experimental studies appear to support the picture of alternate and periodic plume emissions,[58–61] there has been suggestons that periodic plume emission is not necessary for the horizontal oscillation of the bulk fluid.[54,56] Part of the reason for this controversy is that most of the earlier measurements are two-dimensional. To unlock the intricate dynamics of the LSC oscillation, Xi et al.[62] designed a 3D experiment that directly measured the plume oscillation signals simultaneously from the top and bottom plates as well as at the mid-height plane. From these measurements they were able to determine the phase relationships between plume emissions from the top and bottom plates and also plume emissions/arrivals in different regions of the same plate. Their results show convincingly and conclusively that thermal plumes are emitted neither periodically nor alternately, but randomly and continuously, from the top and bottom plates. Their experiment also discovered a new flow mode — the sloshing mode of the LSC, which are shown in Fig. 5. Zhou et al.[63] further discovered

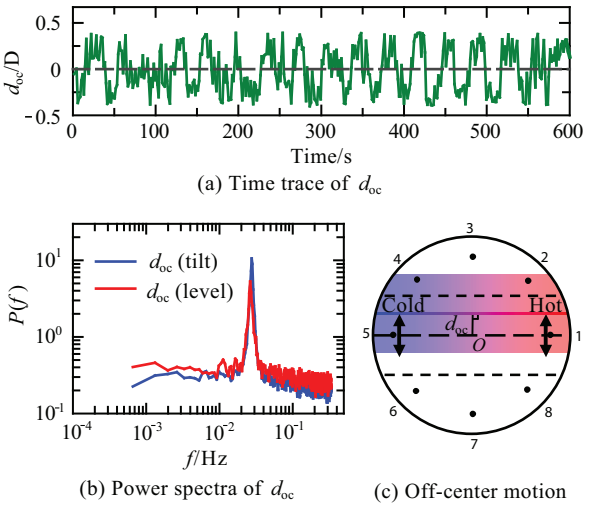

(a) Time trace of d_{oc}

(b) Power spectra of d_{oc} (c) Off-center motion

Fig. 5. The sloshing motion of the LSC as characterized by the quantity d_{oc} (off-center distance), which is defined as the distance between the cell center and the center of the line connecting the hottest and coldest azimuthal positions in the LSC. Plot (c) is a schematic drawing of the off-center motion of the LSC at mid-height plane. The shaded band represents an instantaneous position of the horizontal cross-section of the LSC with its center at a distance d_{oc} away from its average position (long-dashed line), and the two short-dashed lines represent the average position of the LSC band. The black dots represent the 8 thermistors used to measure the sloshing motion.[62] (Figure taken from Ref. 62)

that the sloshing mode at cell center and the torsional mode near the top and bottom plate have a phase difference of $\pi/2$ and are the same oscillatory motion manifested at different heights. This sloshing mode, together with the torsional mode of the LSC, are found to be the origin of the oscillation of the temperature field. Motivated by this discovery, Brown and Ahlers[64] proposed a stochastic model that could explain the origin of the sloshing and torsional oscillations in turbulent convection.

Another intriguing dynamical feature of the LSC is the cessation and reversal phenomenon. It has been observed that the LSC flow strength experiences momentary vanishing, which are called cessations and when, after a cessation, the LSC restarts in an opposite circulation direction, it is called a flow reversal.[65] This phenomenon has attracted a lot of attention since its discovery.[55,65–76]

Besides its importance in understanding the flow dynamics in turbulent convection, this phenomenon is generally believed to have some connection and certain statistical similarity with reversals in the magnetic polarity of the Earth[77] and in the wind direction in the Earth's atmosphere.[78] Its study is therefore of some general interest. Brown et al.[65] made the first systematic studies of the cessation phenomenon in aspect ratio one cylindrical geometry. They found that the LSC is equally likely to restart in any orientation after a cessation, i.e., reversal is only a special case of cessation and that cessation events are Poisson distributed in time, i.e., successive events are uncorrelated. For $\Gamma = 1/2$ case, Xi and Xia[72] found that reversals are more likely to occur after cessations. With the accumulated statistics, they were able to show that, like cessations, reversal events also obey Poisson distribution. For 2D and quasi-2D systems, Sugiyama et al.[74] found that the reversal frequency decreases with increasing Ra, which is in sharp contrast with 3D case where the cessation frequency is found to be independent of Ra. There are a number of theoretical studies aimed at understanding this phenomenon, some are stochastic and some are deterministic. In particular, Brown and Ahlers[79] proposed a model based on physically motivated ordinary differential equations with stochastic noise term and find very good agreement with experimental results. However, a model that can explain the observed phenomena in both 2D and 3D cases under a unified framework is still missing.

B. Thermal plumes

Thermal plumes, both as thermal and geometrical objects, play an important role in heat transport, and there are a number of studies devoted to this subject. For example, using direct and simultaneous local velocity and temperature measurements, Shang et al.[80,81] obtained the local heat flux and found that the thermal plumes are dominant carriers of heat in turbulent convection and that, due to the LSC, the heat flux in the convection cell are mainly transported by plumes along the sidewall of the convection cell. In a later study, Shang et al.[82] further showed that the local heat flux at cell center scales with Ra with an exponent close to 0.5, suggesting that in the turbulent bulk flow, i.e., in the absence of boundary layers, the scaling is similar to that in an ultimate regime, which also confirms the numerical results of Lohse and Toschi[20] for homogenepous RB convection.

Zhou and Xia[83] extracted plumes from the measured temperature time series by recognizing that thermal plumes produce cliff and ramp structures in the measured local temperature time series and using the criterion $T_{\tau_\eta} > T_{\rm rms}$ (where T_{τ_η} is temperature increment over the dissipative timescale). In contrast to "ramp-cliff" structures for passive scalars, these extracted plume signals clearly exhibit "cliff-ramp" structures (corresponding to the cap of plumes) that exhibit log-normal distribution. Zhou et al.,[84] in a later study of morphological transformation from mushroom-like to sheetlike plumes, found that several other properties of plumes, such as the area, circumference and heat content (as shown in Fig. 6), also exhibit log-normal distributions, suggesting that long-normality may be a generic feature of plume-related quantities. In the same study, Zhou et al.[84] also found that plumes in the bulk are always associated with strong vertical vorticity, this finding suggests that mushroomlike plumes are essen-

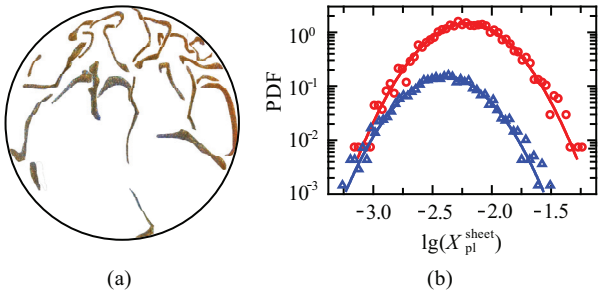

Fig. 6. (a) An example of extracted sheetlike plumes with background in the original image removed. (b) Probability density functions (PDFs) of the logarithm of the normalized sheetlike-plume area and heat content, the horizontal axis label $X_{\rm pl}^{\rm sheet} = A_{\rm pl}^{\rm sheet}/(\pi r^2)$ for circles and $Q_{\rm pl}^{\rm sheet}/Q_0$ for triangles, where $A_{\rm pl}^{\rm sheet}$ and $Q_{\rm pl}^{\rm sheet}$ are the area and "heat content" of the sheetlike plumes, respectively. For clarity, the vertical scale for $\lg(Q_{\rm pl}^{\rm sheet}/Q_0)$ has been divided by 10. The curves are Gaussian-fittings to the respective data.[84] (Figure taken from Ref. 84)

tially vortical structures. Using simultaneously measured local velocity and temperature data,[80] Ching et al.[86] obtained plume velocity by calculating the conditional average of velocity on temperature and decomposed the velocity signal into a sum of plume velocity and a background one that is uncorrelated with the temperature. In direct numerical simulation (DNS) studies, in which velocity and temperature field can be obtained simultaneously, more elaborate plume extraction schemes have been developed. For example, Julien et al.[85] identified plumes using several criteria that are combinations of temperature, vertical velocity and vertical vorticity satisfying certain thresholds. Using such method, they separated the measured local heat flux into the ones carried by the plumes and by the background velocity. While in Zhou et al.[84] individual sheetlike plumes were extracted manually, Shishkina and Wagner[87] identified them using the properties of temperature, thermal dissipation rate and vorticity.

V. SMALL-SCALE THERMAL TURBULENCE

What is the physical mechanism that drives the cascades of the velocity and temperature fields in buoyancy-driven turbulence, such as turbulent thermal convection, has been a long-debated issue. The question essentially is: Does buoyancy explicitly manifest itself in the small-scale behavior of velocity and temperature fields in this type of flows, or it will be the same Kolmogorov-type cascade mechanism that dictates the cascades of turbulent kinetic energy and temperature variances? Specifically, does the Bolgiano–Obukhov scaling (BO59) exist above the so-called Bolgiano scale $\ell_{\rm B}$? Note that BO59 also implies that the temperature is an active scalar, at least in the region and within the range of scales it exists. Over the years a number of experimental and numerical studies of RB convection appear to have observed the BO59 scaling. But many of these studies have very limited scaling range and quite often are obtained in the time or frequency domain. Therefore, to really answer this question, one needs to make direct measurements of the spatial velocity and temperature structure functions instead of inferring them from time-domain data. With the advancement of the particle image velocimetry (PIV) technology, high-resolution measurements of the real-space structure functions (SF) become possible. Sun et al.[88] made the first attempt in this direction by measuring high-resolution velocity and the temperature fields in real space. Using PIV and the multi-thermistor-probe technique, they measured respectively the two-dimensional velocity field and the temperature difference, from which the real-space structure functions of both velocity and temperature were obtained. Sun et al. found that in the central region both velocity and temperature exhibit the same scaling behavior that one would find for the velocity and for a passive scalar in homogeneous and isotropic Navier–Stokes turbulence. On the other hand, Kunnen et al.,[89] also using PIV and also in water-filled cylinder of aspect ratio one but with a Ra number that is approximately ten times smaller than that in Sun et al. Their results for low-order velocity SFs appear to support BO59 scaling, although the scaling range is very short. How can one understand the apparent discrepancy? In the case of Sun et al., the estimated Bolgiano scale is based on the globally averaged viscous and thermal dissipation rates which can be related to the global quantities Ra and Pr by the equations of motion. This result indicates that BO59 should be easier to observe with higher Rayleigh number. However, this is misleading. As the dissipation rates are local quantities or fields and they are not spatially homogeneous as shown in the DNS results by Kunnen et al.[89] In fact what they found was that locally the Bolgiano scale increases with Ra, which is opposite to the behavior of its global counterpart. If one uses the numerical result of Kunnen et al., one sees that the local Bolgiano scale in the case of Sun et al. is ten times larger than the global one and it is also larger than the size of their PIV measurement region. This may explain why Sun et al. observed K41-like scaling, it is the one that one should have expected in the range of scales of their measurement. Now one would conclude that we should look for BO59 scaling using smaller values of Ra. But this will also reduce the inertial range, which one can see already from the results of Kunnen et al. In addition, it has been found much earlier by Calzavarini et al. that the Bolgiano scale is the largest in the cell center and that one should look for BO scaling near cell boundaries. But in this case, other effects like shear will contaminate the results. As discussed by Lohse and Xia,[4] due to the opposite behavior of the global ($\langle \ell_{\rm B} \rangle$) and local ($\ell_{\rm B}(\boldsymbol{x})$) Bolgiano scale with respect to their Ra dependence, and the lack of wide separation of scales between η (the Kolmogorov dissipation scale), $\ell_{\rm B}$

and L (the integral scale), as well as theoretical inconsistencies of the Bolgiano argument itself, the existence of the Bolgiano scale (i.e., BO59-type of scaling above ℓ_B and K41-type scaling below ℓ_B) remains unsettled.

Because of the space limitation, issues such as the statistical properties of temperature as an active scalar and the mixing of passive scalar in buoyancy-driven flows will not be discussed here.[83,90]

VI. RECENT DEVELOPMENTS

In recent years, research in turbulent thermal convection has gone beyond the classical RB case. These include thermal convection with phase change or multiphase fluids, rotational RB convection.

A. Convection in multiphase fluids

Convection in multiphase fluids has become a very active research topic in recent years, partly because of its potential application in engineering problems such as heat transfer and in meteorology such as in cloud physics. There are a number of studies that fall under this category. These include convection involving phase change of single component fluids through condensation and evaporation between the vapor and liquid phases,[91,92] convection in fluids with bubbles,[93–95] convection in nanofluids,[96] convection with polymer additives,[97–99] and moist convections.[100–102] In an experimental study involving the evaporation and condensation of ethane, Zhong et al.[91] found that the effective thermal conductivity is increased over one order of magnitude that of single phase. In several numerical studies, it was found that the introduction of micro-sized bubbles, either introduced externally or through boiling, into RB convection can greatly increase the Nu by almost an order of magnitude.[92–94] On the other hand, adding nano-sized conducting particles (nanofluids)[96] or small amount of polymers[97] to the standard RB cell have seen reduction of Nu. However, by using rough plates (therefore reducing the contribution of BL to the total dissipation of the system), Wei et al.[98] have found an increase of Nu beyond certain polymer concentration (as shown in Fig. 7). Their results are consistent with the numerical results of Benzi et al.[99] that showed Nu increase with polymers additives in homogeneous RB convection. Together, these results suggest that polymer additives can enhance heat transport when they are in the bulk, but will reduce heat transport when they are in the boundary layer. On the other hand, exactly how polymers can enhance heat transport in the turbulent bulk remains unclear, although there are evidences that the coherence of temperature field are increased with the presence of polymers.[99] This suggests that studying how polymers modify the small-scale properties of the flow, such as turbulent cascades and energy balance, should provide some insight to this very important and intriguing problem. Another example of turbulent convection involving multiphase fluids is moist convection. It has attracted some attention recently because of its close connection to cloud formation in the atmospheres.[100–104] Because of space limit, this very interesting topic will not discussed here.

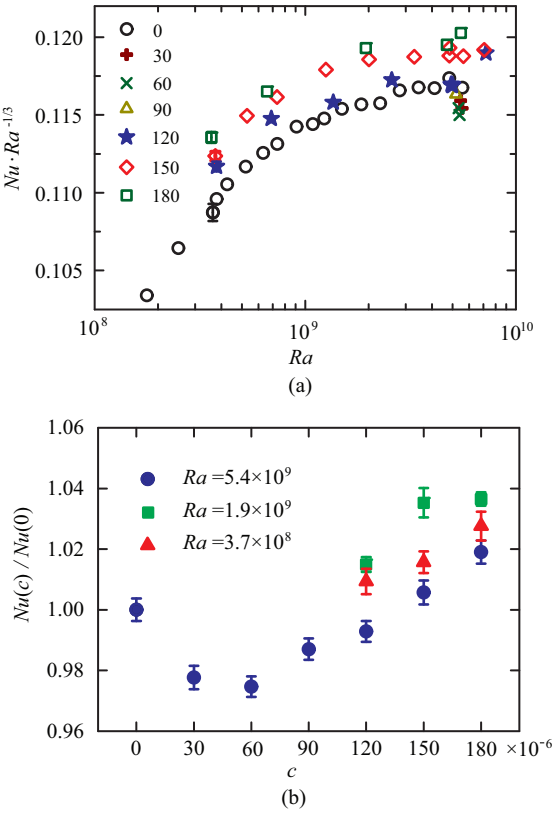

Fig. 7. Enhanced and reduced global heat transport by polymer additives. The experiment was conducted using the polymer polyethylene oxide (PEO) of molecular weight 4×10^6 g/mol in an aspect ratio one cylindrical cell with rough top and bottom plates. (a) Compensated Nu as a function of Ra for polymer concentrations $c = 120$, 150, and 180 ppm (1 ppm $= 1 \times 10^{-6}$). Also shown are compensated Nu measured with c varying from 30 to 180 ppm at approximately the same $Ra \approx 5.4 \times 10^9$. The open circles represent pure fluid result. (b) Nu normalized by pure fluid value versus polymer concentration c for several values of Ra.[98] (Figure taken from Ref. 98)

B. Rotating Rayleigh–Bénard convection

Rotating RB convection has attracted a lot of attentions in recent years,[105–112] as it is highly relevant for geophysical and astrophysical systems. How rotation influences heat transport and the large scale flow dynamics are some of the questions that have been asked. It has been widely assumed that competition between the global buoyancy force and the Coriolis force is the main factor governing the flow dynamics in rotating convection. A coupled set of laboratory and numeri-

cal works by King et al.[109,110] showed that the global force balance argument could not correctly predict the crossover between different regimes. Instead, they argued that whether the flow is in one regime or the other depends on the relative thicknesses of thermal and Ekman boundary layers. Ekman pumping has been attributed to the observed heat transport enhancement in experiment. For example, Zhong et al.[107,108] have found in an experimental study that under an appropriate range of parameters (Ra, Pr, and the rotation rate), Nu can be enhanced by unto 30% due to the stretching of plumes from the BL by Ekman pumping. On the other hand, no direct measurement of the Ekman layer has ever been made and the exact nature of Ekman pumping remains unclear. This points to a future direction of research in the area of rotating convection.

C. Convection in multilayer fluids

Another area of non-standard RB convection involves multilayer fluids. Multilayer turbulent flow, in particular, multilayer turbulent convection is a phenomenon occurring widely in nature. An example is the coupled system of atmospheric and oceanic convections, in which convection is either thermally driven or density driven. Recently, Xie and Xia[113] made an experimental investigation of the flow dynamics in a two-layer RB convection (as shown in Fig. 8). They found that there exists one LSC in each layer and the two can couple in two different modes, viscous coupling (the two LSCs are in the same direction at the interface) and the thermal coupling (the two are opposite to each other at the interface). Furthermore, the cessation/reversal behaviors in the two-layer system are dynamically distinct from those in single-layer RB convection. This preliminary study suggests that there are rich dynamical behaviors to be explored in multilayer turbulent convection.

D. Geometrical and confinement effects in turbulent convection

The ability to significantly enhance the efficiency of heat transfer is of great importance in industry and in many daily applications. In many engineering applications heat transfer often take place in confined spaces, such as cooling in microelectronic devices. However, turbulent convection in highly confined geometries have been seldom studied. Recently, there have been a number of studies in this direction. For example, Poel et al.[114] made a numerical study of aspect ratio dependence in a 2D system. Zhou et al.[29] made an experimental study of the aspect ratio dependence in rectangular geometry with aspect ratios $\Gamma_\perp$ ($\Gamma_\perp = W/H$) in the plane perpendicular to the LSC's circulation plane as small as 0.3. Note that reducing $\Gamma_\perp$ decreases the separation between the front and back walls of the convection cell and increases the effect of confinement, which

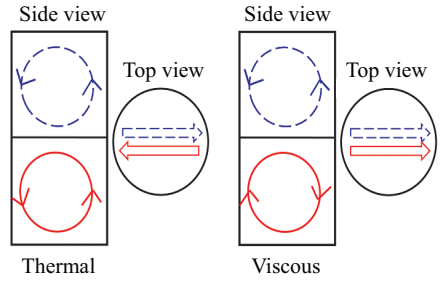

(a) Schematics of the two flow-coupling modes

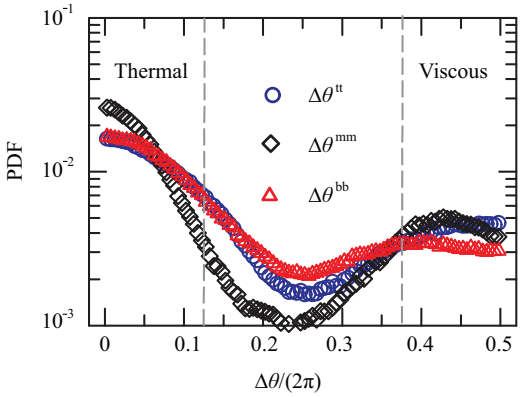

(b) Probability density function of $\Delta\theta$

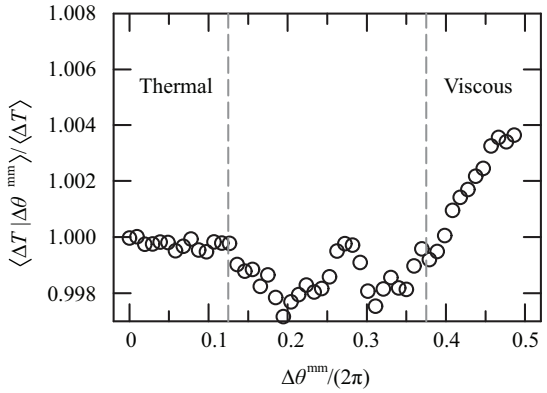

(c) Normalized temperature difference of the top and bottom plates

Fig. 8. Flow couplings in two-layer turbulent convection. $\Delta\theta$ in plot (b) stands for difference between the azimuthal orientations (phase difference) of the LSCs in the two layers and "t", "m" and "b" stand for the top and middle and bottom positions of the LSC. (c) Normalized temperature difference of the top and bottom plates conditioned on the flow coupling parameter $\Delta\theta^{mm}$, which shows that thermal coupling is more efficient for heat transport than viscous coupling in the two-layer thermal convection system. The dashed lines are the boundaries for different coupling states. Thermal and viscous stand for thermal coupling and viscous coupling, respectively.[113] (Figure taken from Ref. 113)

should increase the frictional drag from the walls. With increased frictional drag from the container walls, one would ordinarily expect decreased transport of these quantities. Therefore, it came as a big surprise when Huang et al.[31] observed heat transfer enhancement by narrowing the width of a RB convection cell. Their

study shows that, as expected, the increased drag from the confining walls indeed decreases the turbulent flow velocity, therefore reducing momentum and mass transport. The heat transport also decreases initially with decreasing aspect ratio. But when $\Gamma_\perp$ becomes smaller than 0.3, the global Nu increases significantly, apparently offsetting the effect of drag increase. Their detailed experimental and numerical investigations show that the confinement also changes the dynamics and morphology of thermal plumes such that these heat-carrying objects become more coherent. As a result, these plumes experience less heat loss as they travel across the convection cell, which led to a net increase of heat transfer efficiency. For the parameter range explored, they found that Nu is increased by up to 17%. As shown in Fig. 9, unlike in the large aspect ratio ($\Gamma \sim 1$) case, where heat are mainly transported along the perimeter of the cell by plumes carried by the LSC, in the confined (small Γ) cases, plumes are more coherent and go up and down vertically in random locations. The study demonstrates how changes in turbulent bulk flow can influence the boundary layer dynamics and shows that the prevalent mode of heat transfer existing in larger aspect ratio convection cells, in which hot and cold thermal plumes are carried by the LSC along opposite sides of the sidewall, is not the most efficient way for heat transport. The study sheds new light on turbulent heat transport and has potential applications in passive heat management, which is critical for many microelectronic devices.

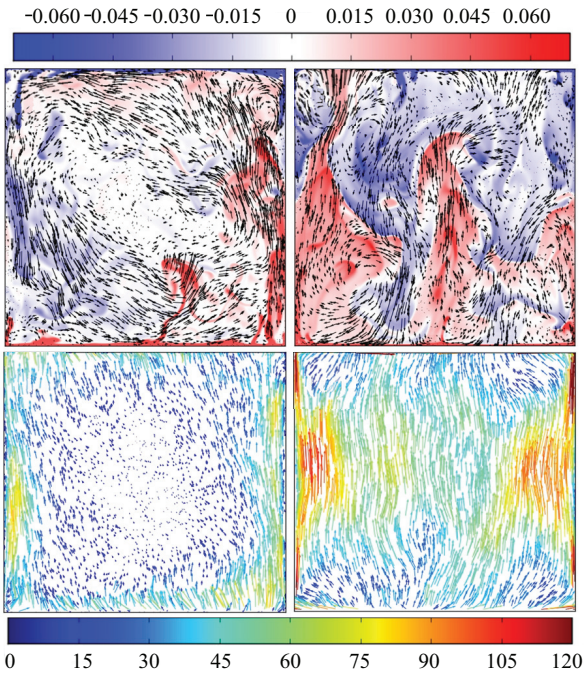

Fig. 9. Instantaneous temperature-velocity fields (top panel) and time-averaged local heat flux (bottom panel) in the vertical x-z plane mid-way between the lateral y-walls for $\Gamma = 1/2$ (left) and $\Gamma = 1/8$ (right). These figures illustrate how geometric confinement changes the paradigmatic mode of heat transfer in turbulent convection. In large aspect ratio (~ 1) geometries the LSC carries hot and cold plumes along opposite sidewalls in a circulatory motion. In confined geometries (small aspect ratios), more coherent plumes go up and down vertically in random locations. The temperature is coded in color in the unit of ΔT such that it is zero at cell center, and the velocity is coded in vector length in unit of free-fall velocity. The non-dimensional heat flux is coded in both color scale and vector length.[31] (Figure taken from Ref. 31)

VII. FUTURE DIRECTIONS

From the above examples, we can see that one of the future trends in turbulent thermal convection research is that investigations will be carried out in non-standard RB configurations that are more directly related to many of the "real world" problems in geophysics, astrophysics and engineering applications. On the other hand, the classical RB convection still is the canonical system for understanding the generic thermal convection problem because of its simplicity, i.e., well-defined boundary conditions and precisely-tunable control parameters. In fact, several major issues remain for the RB system. The first one regards the existence and nature of the ultimate regime. As already discussed, although there are evidences to show the existence of or transition to this state. This has not been accepted by the entire convection community. This is partly because of the Ra range is rather short. Future efforts should be made to extend the Ra range of the observed regime and, perhaps more importantly, to directly probe the associated boundary layer transitions. The second question regards the existence of the BO scaling. Here existence means not just some power laws that have exponents that are the same as predicted by BO59, but the scaling should be observed over an extended, and the same, range of spatial scales for both the velocity and temperature above the Bolgiano scale. As already stated, this question is of fundamental importance. Even if it exists, the range of scales for this scaling is likely to be very short. Therefore, direct test of the force balance assumption that underlies the BO scaling[4] should provide more conclusive results. Note that this assumption was recently validated numerically in 2D Rayleigh–Taylor turbulence.[115] The third one is the large-scale circulation. How to understand its rich dynamics in a coherent way? Some of these are stochastic (like the azimuthal motion, and cessations and reversals); and some appear to be deterministic, like the twisting and sloshing motions. How to describe all of these in a single model based on the equations of motion? Another important question is whether the LSC can persist to extremely high values of Ra, say beyond 10^{14}. And what will happen to the heat transport and other global properties of the system when the LSC does break down?

Because of the space limit, I have to leave out many other interesting topics such as Langrangian measure-

ments. Progress in the Lagrangian studies of turbulent RB convection have been made in recent years, both experimentally and numerically, this allows more direct study of mass transport and particle dispersions in buoyancy-driven turbulent flows.[116–120] Some of the other interesting topics include double diffusive convection and horizontal convection (both are highly relevant to oceanography); convection in highly viscous and non-Boussinesq fluids that are relevant to mantle convection. Through this short (and unavoidable incomplete and biased by personal views), I wish to convey the message that despite over one hundred years of research, RB convection is still a very active and important topic that underlies a wide range of thermally-driven turbulent flows, with much more remain to be explored.

The author would like to thank all his collaborators and colleagues in the field, for the many enjoyable collaborations and stimulating and helpful discussions over the years. In particular, he is indebted to his former as well as current students and postdocs, whose ingenuities and passion for research have made his own such an enjoyable experience. It has been a privilege to work with so many talented and outstanding individuals. This work was supported by the Research Grants Council of Hong Kong, in particular through the General Research Funds (CUHK403811 and CUHK403712), and through the NSFC/RGC Joint Research Scheme (N_CUHK462/11).

1. E. D. Siggia, Ann. Rev. Fluid Mech. **26**, 137 (1994).
2. L. P. Kadanoff, Phys. Today **54**, 34 (2001).
3. G. Ahlers, S. Grossmann, and D. Lohse, Rev. Mod. Phys. **81**, 503 (2009).
4. D. Lohse and K. Q. Xia, Ann. Rev. Fluid Mech. **42**, 335 (2010).
5. F. Chillà and J. Schumacher, Eur. Phys. J. E **35**, 58 (2012).
6. Q. Zhou and K. Q. Xia, Advances in Mechanics **42**, 231 (2012).
7. S. Grossmann and D. Lohse, J. Fluid Mech. **407**, 27 (2000).
8. S. Grossmann and D. Lohse, Phys. Rev. Lett. **86**, 3316 (2001).
9. S. Grossmann and D. Lohse, Phys. Rev. E **66**, 016305 (2002).
10. S. Grossmann and D. Lohse, Phys. Fluids **16**, 4462 (2004).
11. R. H. Kraichnan, Phys. Fluids **5**, 1374 (1962).
12. B. Castaing, G. Gunaratne, F. Heslot, et al., J. Fluid Mech. **204**, 1 (1989).
13. X. Chavanne, F. Chillà, B. Castaing, et al., Phys. Rev. Lett. **79**, 3648 (1997).
14. J. J. Niemela, L. Skrbek, K. R. Sreenivasan, et al., Nature **404**, 837 (2000).
15. X. He, D. Funfschilling, H. Nobach, et al., Phys. Rev. Lett. **108**, 024502 (2012).
16. G. W. He and J. B. Zhang, Phys. Rev. E **73**, 055303(R) (2006).
17. G. W. He and X. Zhao, Phys. Rev. E **79**, 046316 (2009).
18. X. Z. He, G. W. He, and P. Tong, Phys. Rev. E **81**, 065303(R) (2010).
19. Q. Zhou, C. M. Li, Z. M. Lu, et al., J. Fluid Mech. **683**, 94 (2011).
20. D. Lohse and F. Toschi, Phys. Rev. Lett. **90**, 034502 (2003).
21. B. I. Shraiman and E. D. Siggia, Phys. Rev. A **42**, 3650 (1990).
22. G. Ahlers and X. Xu, Phys. Rev. Lett. **86**, 3320 (2001).
23. K. Q. Xia, S. Lam, and S. Q. Zhou, Phys. Rev. Lett. **88**, 064501 (2002).
24. R. du Puits, C. Resagk, and A. Thess, Phys. Rev. E **75**, 016302 (2007).
25. C. Sun, Y. H. Cheung, and K. Q. Xia, J. Fluid Mech. **605**, 79 (2008).
26. D. Funfschilling, E. Brown, A. Nikolaenko, et al., J. Fluid Mech. **536**, 145 (2005).
27. A. Nikolaenko, E. Brown, D. Funfschilling, et al., J. Fluid Mech. **523**, 251 (2005).
28. C. Sun, L. Y. Ren, H. Song, et al., J. Fluid Mech. **542**, 165 (2005).
29. Q. Zhou, B. F. Liu, C. M. Li, et al., J. Fluid Mech. **710**, 260 (2012).
30. Q. Zhou, H. Lu, B. F. Liu, et al., Sci. China-Phys. Mech. Astron. **56**, 989 (2013).
31. S. D. Huang, M. Kaczorowski, R. Ni, et al., Phys. Rev. Lett. **111**, 104501 (2013).
32. K. Q. Xia, Y. B. Xin, and P. Tong, J. Opt. Soc. Am. A **12**, 1571 (1995).
33. Y. B. Xin, K. Q. Xia, and P. Tong, Phys. Rev. Lett. **77**, 1266 (1996).
34. X. L. Qiu and K. Q. Xia, Phys. Rev. E **58**, 5816 (1998).
35. P. Wei and K. Q. Xia, J. Fluid Mech. **720**, 140 (2013).
36. R. du Puits, C. Resagk, and A. Thess, Phys. Rev. Lett. **99**, 234504 (2007).
37. Q. Zhou and K. Q. Xia, Phys. Rev. Lett. **104**, 104301 (2010).
38. Q. Zhou, R. J. A. M. Stevens, K. Sugiyama, et al., J. Fluid Mech. **664**, 297 (2010).
39. Q. Zhou, K. Sugiyama, R. J. A. M. Stevens, et al., Phys. Fluids **23**, 125104 (2011).
40. R. J. A. M. Stevens, Q. Zhou, S. Grossmann, et al., Phys. Rev. E **85**, 027301 (2012).
41. N. Shi, M. S. Emran, and J. Schumacher, J. Fluid Mech. **706**, 5 (2012).
42. J. D. Scheel, E. Kim, and K. R. White, J. Fluid Mech. **711**, 281 (2012).
43. L. Li, N. Shi, R. du Puits, et al., Phys. Rev. E **86**, 026315 (2012).
44. H. D. Xi, S. Lam, and K. Q. Xia, J. Fluid Mech. **503**, 47 (2004).
45. X. L. Qiu and P. Tong, Phys. Rev. E **66**, 026308 (2002).
46. C. Sun and K. Q. Xia, Phys. Rev. E **72**, 067302 (2005).
47. J. J. Niemela and K. R. Sreenivasan, Europhys. Lett. **62**, 829 (2003).
48. X. L. Qiu, S. H. Yao, and P. Tong, Phys. Rev. E **61**, R6075 (2000).
49. X. D. Shang and K. Q. Xia, Phys. Rev. E **64**, 065301 (2001).
50. T. Takeshita, T. Segawa, J. A. Glazier, et al., Phys. Rev. Lett. **76**, 1465 (1996).
51. E. Brown, D. Funfschilling, and G. Ahlers, J. Stat. Mech. **10**, P10005 (2007).
52. J. J. Niemela and K. R. Sreenivasan, J. Fluid Mech. **557**, 411 (2006).
53. S. Q. Zhou, C. Sun, and K. Q. Xia, Phys. Rev. E **76**, 036301 (2007).
54. D. Funfschilling and G. Ahlers, Phys. Rev. Lett. **92**, 194502 (2004).
55. H. D. Xi, Q. Zhou, and K. Q. Xia, Phys. Rev. E **73**, 056312 (2006).
56. C. Resagk, R. du Puits, A. Thess, et al., Phys. Fluids **18**, 095105 (2006).
57. E. Villermaux, Phys. Rev. Lett. **75**, 4618 (1995).
58. C. Ciliberto, S. Cioni, and C. Laroche, Phys. Rev. E **54**, R5901 (1996).
59. X. L. Qiu and P. Tong, Phys. Rev. Lett. **87**, 094501 (2001).

60. Y. Tsuji, T. Mizuno, T. Mashiko, et al., Phys. Rev. Lett. **94**, 034501 (2005).
61. C. Sun, K. Q. Xia, and P. Tong, Phys. Rev. E **72**, 026302 (2005).
62. H. D. Xi, S. Q. Zhou, Q. Zhou, et al., Phys. Rev. Lett. **102**, 044503 (2009).
63. Q. Zhou, H. D. Xi, S. Q. Zhou, et al., J. Fluid Mech. **630**, 367 (2009).
64. E. Brown and G. Ahlers, J. Fluid Mech. **638**, 383 (2009).
65. E. Brown, A. Nikolaenko, and G. Ahlers, Phys. Rev. Lett. **95**, 084503 (2005).
66. J. J. Niemela, L. Skrbek, K. R. Sreenivasan, et al., J. Fluid Mech. **449**, 169 (2001).
67. K. R. Sreenivasan, A. Bershadskii, and J. J. Niemela, Phys. Rev. E **65**, 056306 (2002).
68. C. Sun, H. D. Xi, and K. Q. Xia, Phys. Rev. Lett. **95**, 074502 (2005).
69. R. Benzi, Phys. Rev. Lett. **95**, 024502 (2005).
70. F. F. Araujo, S. Grossmann, and D. Lohse, Phys. Rev. Lett. **95**, 084502 (2005).
71. E. Brown and G. Ahlers, J. Fluid Mech. **568**, 351 (2006).
72. H. D. Xi and K. Q. Xia, Phys. Rev. E **75**, 066307 (2007).
73. M. Breuer and U. Hansen, Europhys. Lett. **86**, 24004 (2009).
74. K. Sugiyama, R. Ni, R. J. A. M. Stevens, et al., Phys. Rev. Lett. **105**, 034503 (2010).
75. T. Yanagisawa, Y. Yamagishi, and Y. Hamano, Phys. Rev. E **83**, 036307 (2011).
76. M. Chandra and M. K. Verma, Phys. Rev. Lett. **110**, 114503 (2013).
77. G. A. Glatzmaier, R. S. Coe, L. Hongre, et al., Nature **401**, 885 (1999).
78. E. van Doorn, B. Dhruva, K. R. Sreenivasan, et al., Phys. Fluids **12**, 1529 (2000).
79. E. Brown and G. Ahlers, Phys. Rev. Lett. **98**, 134501 (2007).
80. X. D. Shang, X. L. Qiu, P. Tong, et al., Phys. Rev. Lett. **90**, 074501 (2003).
81. X. D. Shang, X. L. Qiu, P. Tong, et al., Phys. Rev. E **70**, 026308 (2004).
82. X. D. Shang, P. Tong, and K. Q. Xia, Phys. Rev. Lett. **100**, 244503 (2008).
83. S. Q. Zhou and K. Q. Xia, Phys. Rev. Lett. **89**, 184502 (2002).
84. Q. Zhou, C. Sun, and K. Q. Xia, Phys. Rev. Lett. **98**, 074501 (2007).
85. K. Julien, S. Legg, J. McWilliams, et al., J. Fluid Mech. **391**, 151 (1999).
86. E. S. C. Ching, H. Guo, X. D. Shang, et al., Phys. Rev. Lett. **93**, 124501 (2004).
87. O. Shishkina and C. Wagner, J. Fluid Mech. **599**, 383 (2008).
88. C. Sun, Q. Zhou, and K. Q. Xia, Phys. Rev. Lett. **97**, 144504 (2006).
89. R. P. J. Kunnen et al, Phys. Rev. E **77**, 016302 (2008).
90. Q. Zhou and K. Q. Xia, Phys. Rev. E **77**, 056312 (2008).
91. J. Q. Zhong, D. Funfschilling and G. Ahlers, Phys. Rev. Lett. **102**, 124501 (2009).
92. L. Biferale, P. Perlekar, M. Sbragaglia, et al., Phys. Rev. Lett. **108**, 104502 (2012).
93. R. Lakkaraju, R. J. A. M. Stevens, P. Oresta, et al., Proc. Nati. Acad. Sci. **110**, 9237 (2013).
94. P. Oresta, R. Verzicco, D. Lohse, et al., Phys. Rev. E **80**, 026304 (2009).
95. L. E. Schmidt, P. Oresta, F. Toschi, et al., N. J. Phys. **13**, 025002 (2011).
96. R. Ni, S. Q. Zhou, and K. Q. Xia, Phys. Fluids **23**, 022005 (2011).
97. G. Ahlers and A. Nikolaenk, Phys. Rev. Lett. **104**, 034503 (2010).
98. P. Wei, R. Ni, and K. Q. Xia, Phys. Rev. E **86**, 016325 (2012).
99. R. Benzi, E. S. C. Ching, and E. De Angelis, Phys. Rev. Lett. **104**, 034503 (2010).
100. O. Pauluis and J. Schumacher, Comm. Math. Sci. **8**, 295 (2010).
101. T. Weidauer, O. Pauluis, and J. Schumacher, N. J. Phys. **12**, 105002 (2010).
102. O. Pauluis and J. Schumacher, Proc. Nati. Acad. Sci. **108**, 12623 (2011).
103. Z. Warhaft, Fluid Dyn. Res. **41**, 011201 (2009).
104. E. Bodenschatz, S. P. Malinowski, R. A. Shaw, et al., Science **327**, 970 (2010).
105. R. P. J. Kunnen, H. J. H. Clercx, and B. J. Geurts, Phys. Rev. E **74**, 056306 (2006).
106. R. P. J. Kunnen, H. J. H. Clercx, and B. J. Geurts, Europhys. Lett. **84**, 24001 (2008).
107. J. Q. Zhong, R. J. A. M. Stevens, H. J. H. Clercx, et al., Phys. Rev. Lett. **102**, 044502 (2009).
108. R. J. A. M. Stevens, J. Q. Zhong, H. J. H. Clercx, et al., Phys. Rev. Lett. **103**, 024503 (2009).
109. E. M. King, S. Stellmach, J. Noir, et al., Nature **457**, 301 (2009).
110. E. M. King, S. Stellmach, and J. M. Aurnou, J. Fluid Mech. **691**, 568 (2012).
111. E. M. King and J. M. Aurnou, Phys. Rev. E **85**, 016313 (2012).
112. Y. M. Liu and R. E. Ecke, Phys. Rev. E **84**, 016311 (2011).
113. Y. C. Xie and K. Q. Xia, J. Fluid Mech. **728**, R1 (2013).
114. E. P. van der Poel, R. J. A. M. Stevens, and D. Lohse, Phys. Rev. E **84**, 045303 (2011).
115. Q. Zhou, Phys. Fluids **25**, 085107 (2013).
116. J. Schumacher, Phys. Rev. Lett. **100**, 134502 (2008).
117. J. Schumacher, Phys. Rev. E **79**, 056301 (2009).
118. R. Ni, S. D. Huang and K. Q. Xia, Phys. Rev. Lett. **107**, 174503 (2011).
119. R. Ni, S. D. Huang and K. Q. Xia, J. Fluid Mech. **692**, 395 (2012).
120. R. Ni and K. Q. Xia, Phys. Rev. E **87**, 063006 (2013).